

Nanoswitch-based on ring-opening of 1,3-cyclohexadiene molecule

D. Sergeyev^{1*,2}

¹Department of Physics, K. Zhubanov Aktobe Regional State University, Aktobe, Kazakhstan

²Department of Radio Electronics, T. Begeldinov Aktobe Aviation Institute, Aktobe, Kazakhstan

Received 1 May 2020, Accepted 11 December 2020

ABSTRACT

In the framework of the density functional theory, in combination with the method of non-equilibrium Green functions (DFT+NEGF), electric transport characteristics of nanoswitch-based on ring opening of the 1,3-cyclohexadiene molecule (1,3-CHD) are modelled and analyzed. The main electrotransport characteristics (density of states, transmission spectrum, current-voltage characteristics (CVC), dI/dV-characteristics) of a nanoswitch, consisting of Au(111) electrodes forming a nanogap of ~ 10.37 Å, where a 1,3-CHD molecule is placed, upon external exposure of which its rings are opened and turns into a molecule of 1,3,5-hexatriene (1,3,5-HT). The opening of CHD molecule ring noticeably changes the transmission spectrum of the nanodevice: a new peak appears at an energy of 4.4 eV and the width of this peak increases with increasing distance between the ends of the opening σ-bound atoms. An analysis of the transmission spectrum, CVC and dI/dV-characteristics revealed that the 1,3-CHD molecule weakly transmits electric current in the nanosystems under consideration than the 1,3,5-HT molecule. With increasing distance between the final CHD atoms, the slope of the CVC of nanodevices increases, which indicates a decrease in the electrical resistance of the molecule after ring opening. The considered nanoswitch can be used as building blocks for creating logical gates in computer technology.

Keywords: 1,3-cyclohexadiene, 1,3,5-hexatriene, current-voltage characteristics, electrotransport, nanoswitch

1. INTRODUCTION

Recently, intensive studies of the physicochemical properties of various nanostructures has led to the production of materials and devices with new unique characteristics that have made it possible to solve a number of urgent problems both in the field of electronics and in all other areas of science and technology [1, 2]. One of these tasks is the construction of logical gates of computer technology based on nanomaterials, since quantum effects are now actively used for these purposes [3–5]. Logical gates on various materials and new physical principles have already been proposed and created – on carbon nanomaterials (graphene [6, 7], carbon nanotubes [8, 9], fullerenes [10, 11]), on semiconductors [12–14], on heterostructures [15, 16], on superconductors [17–19], on organic nanostructures [20–22] and others.

However, one cannot neglect the logic gates implemented on the old ideas of circuit electronics, which are based on the use of advanced transistor switches [23, 24]. To implement the latter, intensive research is underway to obtain new and effective types of nano-molecular switches [25].

At present, the quantum transport characteristics of individual molecules for creating electronic circuits and devices based on them are of great interest [26–28]. Effective molecular switches are needed to control the operation of such nanocircuits and nanodevices, therefore, an active search is underway for molecules capable of changing the electrical resistance, depending on the external influence (irradiation, heating, electrical, magnetic and chemical effects), behave like a

* Corresponding Author: serdau@mail.ru

conductor (less resistance – the state is on), then like an insulator (high resistance – the state is off). One of the common nanostructures that are candidates for the role of molecular switches is considered to be the molecules of photochromic compounds (spirooxazines, digetariethenes, spirooxazines, azobenzene and others), which are isomerized upon transition to higher excited electronic states as a result of cis-trans isomerization, cyclic transformations and proton photo transfer [29].

In [30–32], the breaking of the cyclic molecule of 1,3-cyclohexadiene (1,3-CHD) and the vibrations of the formed chain of 1,3,5-hexatriene (1,3,5-HT) were studied. In a 1,3-CHD molecule, the two available double bonds are conjugated, that is, separated by only one bond. Under the action of radiation (ultraviolet, X-ray, etc.), the σ -bond opposite the conjugated system breaks; at the same time, the redistribution of the electrons of the double bonds occurs and as a result, an open molecule 1,3,5-HT is formed (Fig. 1). In [33–35], the photochemical reactions of the opening of the 1,3-CHD ring with the formation of 1,3,5-HT were studied and a low quantum yield the ring opening reaction and an attractive interaction between the ends of the fissile CHD σ -bond were revealed, which shows the restoration possibility on the shape of the ring. Such transformations of cyclic molecules are of great interest, since when a molecule ring breaks, its electric transport properties change, as well as structural rearrangements inside the molecules occur at ultrafast time scales, which makes such molecules attractive for creating nanoswitches [36].

In this work, in the framework of the density functional theory in combination with the method of nonequilibrium Green functions (DFT + NEGF), the electric transport characteristics of a nanoswitch based on the conversion of $1,3\text{-CHD} \rightarrow 1,3,5\text{-HT}$ located between gold Au(111) electrodes are modelled and analyzed (Fig. 1).

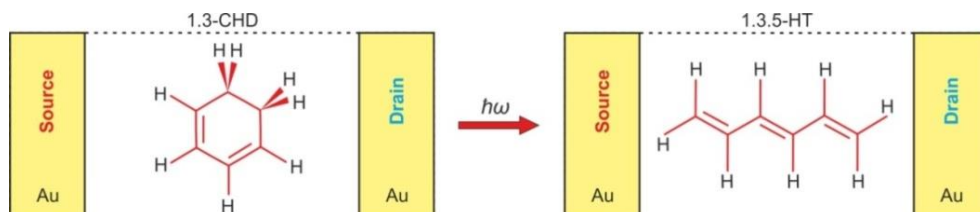


Figure 1. Nanoswitch model based on $1,3\text{-CHD} \rightarrow 1,3,5\text{-HT}$

2. COMPUTATIONAL DETAILS AND BASIC EQUATIONS

The evolution of 1,3-CHD molecule ring breakage is shown in Fig. 2 (for the convenience of describing each configuration, the letters A, B, C, D are conditionally assigned, respectively). In 1,3-CHD (A-configuration), the distance between adjacent hydrogen atoms is ~ 2.54 Å, and between adjacent carbon atoms is ~ 1.51 Å. When the ring of the 1,3-CHD molecule is opened, in the case where the B-configuration between carbon atoms at the rupture site increases to ~ 2.12 Å, and in the C-configuration it increases to ~ 4.03 Å.

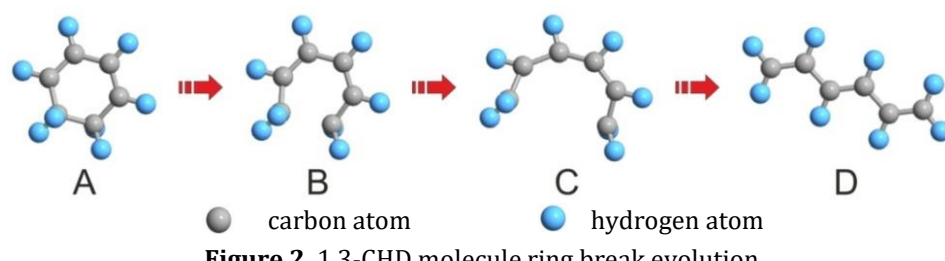


Figure 2. 1,3-CHD molecule ring break evolution

In this work, a nanodevice consisting of gold electrodes (278 atoms) and forming a nanogap with

a size of $\sim 10.37 \text{ \AA}$ is considered as a nano-molecular switch (Fig. 3). A 1,3-CHD molecule is placed in this nanogap, which, after external action (irradiation), begins to open; when it is straightened (after full optimization of the nanostructure), it forms a 1,3,5-HT molecule.

The geometry of the studied nanodevices, in which the A-, B-, C-, D-configurations of the molecule located between the two surfaces of Au(111), is used as the conduction channel is shown on Fig. 3 a-d. The length of the investigated structure is $\sim 41.5 \text{ \AA}$, and the length of the electrodes along the C axis is $\sim 7.06 \text{ \AA}$. The distance between the two electrodes is about 27.38 \AA . The size of the scattering region of quasiparticles is comparable with size of the molecules of 1,3-CHD and 1,3,5-HT. In the configurations under consideration, the distance from the Au(111) surfaces to the molecule varies from $\sim 2.9 \text{ \AA}$ (A-configuration) to $\sim 2.1 \text{ \AA}$ (D-configuration).

The geometry optimization procedure for the nanostructures under consideration and the interatomic interaction description were carried out in the framework of the DFT; the generalized gradient approximation GGA-PBE was used as the exchange-correlation functional [37, 38], which allows the most accurate description of such structures. The structure of the A-, B-, C-, D-configurations and the distance between atoms and electrodes are completely weakened until the forces on the atoms of the molecule become less than 0.02 eV/\AA , and the gold atoms are fixed in their bulk positions (Fig. 3).

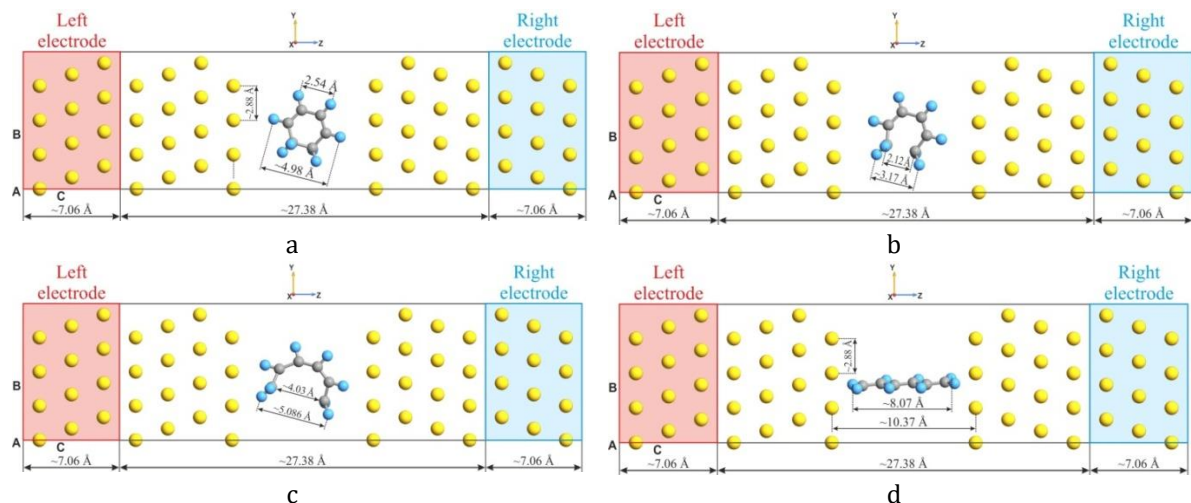


Figure 3. Geometry of nanodevices with A-, B-, C-, D-configurations

Computer simulation representing the electrical characteristics of the nanostructure was carried out in the framework of the DFT using the method of NEGF in the local density approximation (LDA) [39–41]. The simulation of the quantum transport characteristics of a nanostructure is implemented in the Atomistix ToolKit with Virtual NanoLab program [42] (basic equations of this method are described in detail in [43–45]). To calculate the CVC and differential conductivity, the transmission spectrum (function) $T(\varepsilon)$ of the considered nanodevice is first determined:

$$T(\varepsilon) = \text{tr}[\Gamma^L G \Gamma^R G^\dagger] = \text{tr}[\Gamma^R G \Gamma^L G^\dagger] \quad (1)$$

where $\Gamma^{L(R)}(\varepsilon)$ is the broadening matrix (broadening function) of the left (right) electrode, $G(\varepsilon)$, $G^\dagger(\varepsilon)$ are the retarded and advanced Green functions respectively and ε is the energy. The CVC of a nanostructure is calculated on the basis of the well-known Landauer equation, which indicates the fundamental relationship of the electric current with the transmission spectrum [46]:

$$I(V_L, V_R, T_L, T_R) = \frac{2e}{h} \int_{-\infty}^{+\infty} T(\varepsilon) \left[f\left(\frac{\varepsilon - \mu_R}{k_B T_R}\right) - f\left(\frac{\varepsilon - \mu_L}{k_B T_L}\right) \right] d\varepsilon \quad (2)$$

where e is the electron charge, h is the Planck constant, $f(\varepsilon)$ is the Fermi energy distribution

function of quasiparticles, k_B is the Boltzmann constant, T_R , T_L are the current temperatures and μ_R , μ_L are the electrochemical potentials of the right and left electrode.

Note that the molecule is connected with two gold contacts capable of restoring equilibrium in the process of electron transport.

The differential conductivity of the nanostructure was obtained by calculating a self-consistent current for a number of applied biases and performing numerical differentiation:

$$\sigma(V_{bias}, T_L, T_R) = \frac{I(V_{bias}^1, T_L, T_R) - I(V_{bias}^2, T_L, T_R)}{V_{bias}^1 - V_{bias}^2} \quad (3)$$

To determine the density of state of a nanodevice, we first calculate its local density of states (LDOS):

$$D(\varepsilon, r) = \sum_{ij} \rho_{ij}(\varepsilon) \phi_i(r) \phi_j(r) \quad (4)$$

where $\rho(\varepsilon) = \rho^L(\varepsilon) + \rho^R(\varepsilon)$, $\phi(r)$ are the basic orbitals. The DOS of a nanodevice is obtained by integrating LDOS over the entire space:

$$D(\varepsilon) = \int dr D(\varepsilon) = \sum_{ij} \rho_{ij}(\varepsilon) S_{ij} \quad (5)$$

where $S_{ij} = \int \phi_i(r) \phi_j(r) dr$ is the overlap matrix.

3. RESULTS AND DISCUSSION

The results of the calculation of the density of states of a nanodevice (DDOS) with various molecular configurations are presented in Fig. 4. The DOS calculation is based on equations (4, 5). As can be seen, with positive energy on DOS, no significant changes are observed, and with negative energy, changes in DOS occur in intermediate B-, C-configurations.

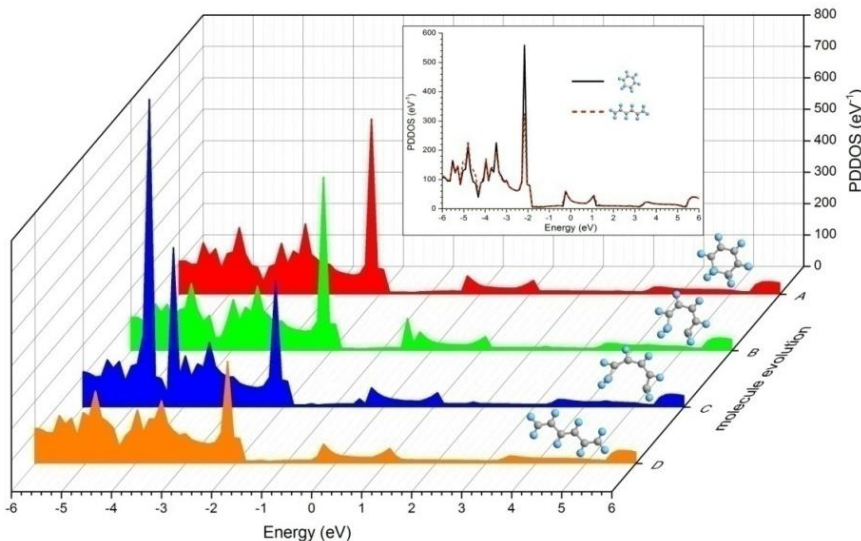


Figure 4.DOS of the nanodevice “Au – (1,3-CHD→ 1,3,5-HT) – Au”

After ring breaking near the Fermi energy in the B- and C-configurations, DOS peak is observed, which disappears after the molecule is straightened (1,3,5-HT). From the breaking of a molecule's ring (A-configuration) to its straightening (D-configuration) at an energy of ~-2.2 eV, the DOS peak decreases from ~ 559 eV⁻¹ to ~ 325 eV⁻¹, respectively, with B-, C-configurations of DOS takes the values of ~ 553 eV⁻¹ and ~ 403 eV⁻¹.

At negative energy, the DOS structure of C-configuration is noticeably different from the others:

2 peaks of DOS 980.58 eV^{-1} and 508.1 eV^{-1} appear at energies of -4.68 eV and -4.2 eV , respectively, associated with the structural transformations of the molecule. At energies $\varepsilon \approx -0.24 \text{ eV}$ and $\varepsilon \approx 1.08 \text{ eV}$, DOS peaks appear in all configurations under consideration, ranging from 59.4 eV^{-1} to 62 eV^{-1} and from 44.92 eV^{-1} to 47.56 eV^{-1} , respectively. Note that in addition to these characteristic peaks, the DOS features of the B- and C-configurations of 102.97 eV^{-1} and 25.82 eV^{-1} arise at an energy of -0.48 eV , associated with unstable atomic positions, which still minimize their energies.

The transmission spectra of the nanodevices at zero bias voltage calculated according to equation (1) are presented in Fig. 5. It is known that the more peaks in the transmission spectrum, the higher the indices of the transport of quasiparticles through the molecule. As you can see, the electric transport of nanodevices with A- and B-configuration is worse than others. For example, a nanodevice with an A-configuration transmits quasiparticles only at energies of -5.5 eV , -3.4 eV , -3 eV . After a molecule ring breaks, significant changes are observed in the transmission spectrum: a new peak appears at 4.4 eV , and with increasing distance of the breaking atoms, the width of this peak increases.

The characteristic features of DOS in the form of a two-peak structure is also manifested in the transmission spectrum, since these values are directly proportional, i.e. $T(\varepsilon) = D(\varepsilon - U)2\pi\gamma_1\gamma_2/\gamma$, here, U is the self-consistent potential, γ is the Luttinger parameter [47]. Before ring breaking, these features are weakly manifested at energies of $\sim -0.6 \text{ eV}$ and 2.8 eV , and after the breaking and an increase in the interatomic distance at the ring opening site, the distance between these peaks decreases and the transmission ability of the molecule increases. For example, after breaking (B-configuration), these features arise at $\sim -0.4 \text{ eV}$ and 2.3 eV , and in the C-configuration at 0.1 eV and 1.8 eV , when the structure is straightened, these peaks merge after full optimization.

The peak of the transmission spectrum (at an energy of $\sim -5.5 \text{ eV}$) decreases when the molecule's ring breaks, and then, when the structure is straightened(after optimization), increases.

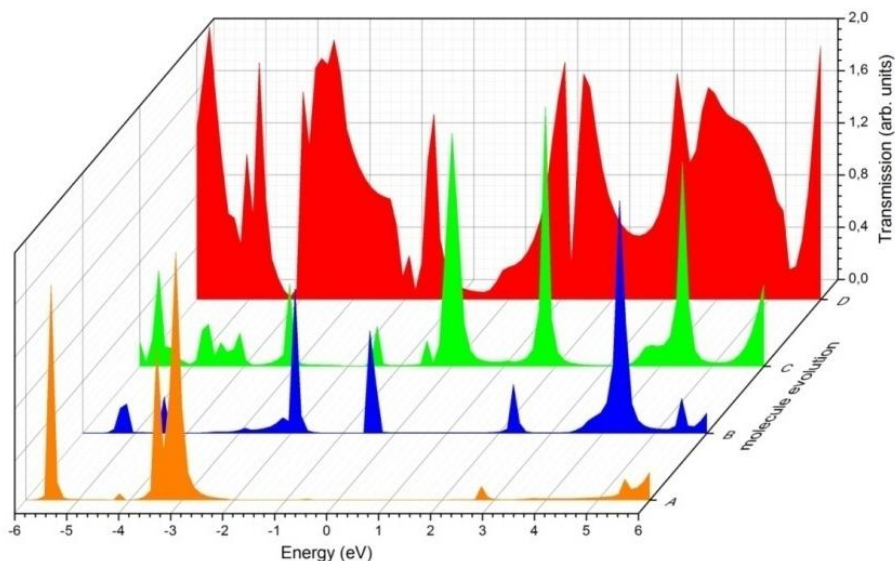


Figure 5.Nanodevice transmission spectrum “Au – (1,3-CHD → 1,3,5-HT) – Au”

Fig.6 presents information on the various contributions of different atoms of the A-, B-, C- and D-configuration of the molecule to local density of states (LDOS). As can be seen, the LDOS Au(111) profile during structural transformations of the $1,3\text{-CHD} \rightarrow 1,3,5\text{-HT}$ molecule does not change. However, a change in the LDOS value of Au(111) layers is observed, which are located near the CHD and HT molecules. These changes are explained by the interaction of surface Au atoms with CHD and HT atoms. In nanosystems with A-, B- and D-configuration molecules, we observe a quasi-uniform distribution of LDOS (Fig. 6, a, b, d, for clarity, we show the increased LDOS

profiles). LDOS molecules of the C-configuration are of great importance relative to others, associated with structural changes during straightening. A cluster of atoms of an under-optimized structure is observed near the center of the nanodevice: 4 peaks of LDOS $35.3 \text{ eV}^{-1}\text{\AA}^{-3}$, $51 \text{ eV}^{-1}\text{\AA}^{-3}$, $107.46 \text{ eV}^{-1}\text{\AA}^{-3}$, $67 \text{ eV}^{-1}\text{\AA}^{-3}$ appear at values of ~ 0.4 , 0.43 , 0.54 , 0.58 conv. units, respectively. After the ring opening of the 1,3-CHD molecule, an asymmetry of the nanocontact geometry (configurations B and C) occurs, which is eliminated after minimizing the energy of the structure and completing the conversion of the 1,3-CHD molecule to the 1,3,5-HT molecule. The simulation results of the CVC and differential conductivity are shown in Fig. 7 (CVC and differential conductivity of the nanostructures under consideration were calculated using equations (2, 3)). As can be seen, no current flows through the 1,3-CHD molecule (A-configuration). This is due to the formation of a barrier between the Au(111) electrode and the 1,3-CHD channel, since the distance from the Au(111) surface to the molecule is $\sim 2.9 \text{ \AA}$. Under such conditions, overcoming the barrier by electrons will be difficult.

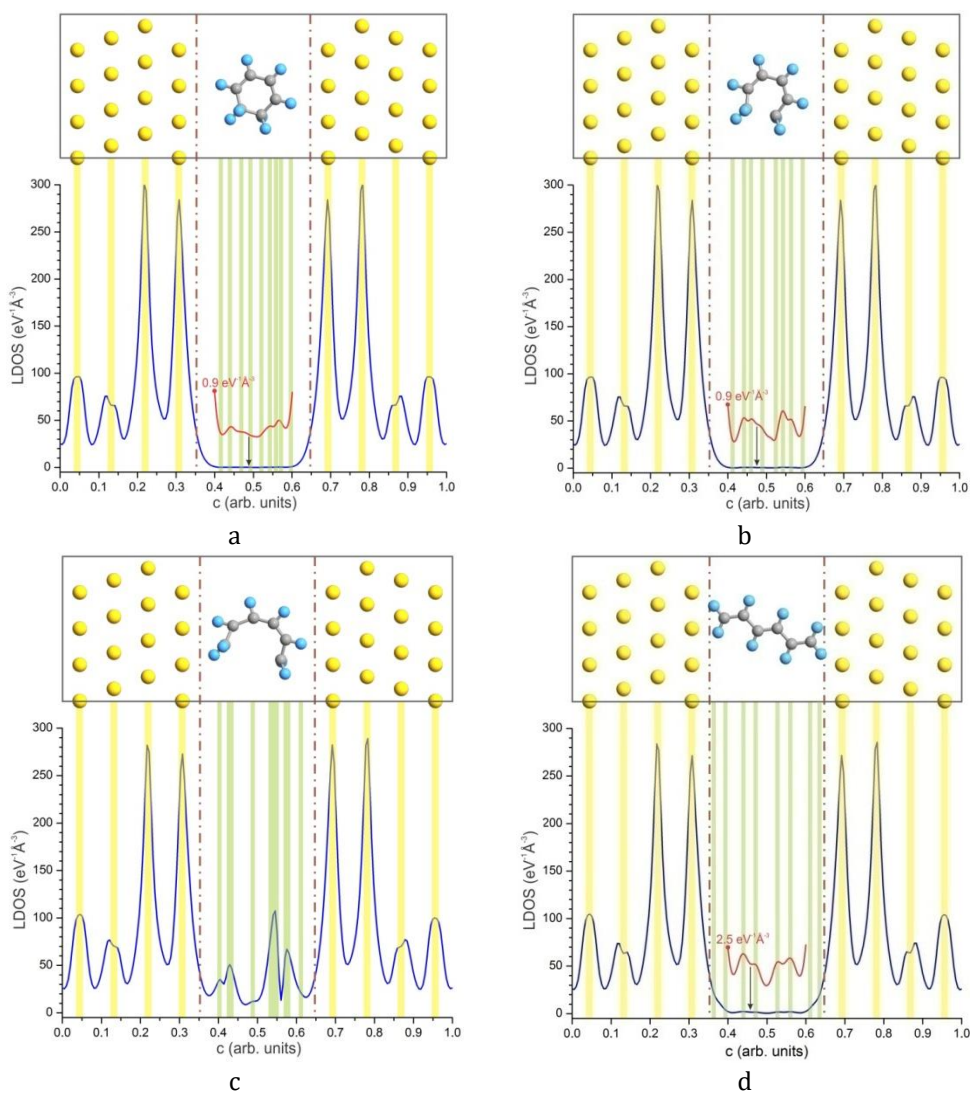


Figure 6. LDOS of “Au – (1,3-CHD → 1,3,5-HT) – Au” nanodevice

A similar process proceeds in a nanostructure with a B-configuration. In the range of $-1.8 \div 2.2 \text{ V}$, practically no current flows through the nanodevice based on the B-configuration. The distance from the Au(111) surface to the molecule is $\sim 2.85 \text{ \AA}$. However, at relatively large positive and negative voltages of $\sim \pm 2 \text{ V}$, we observe an increase in current to $\sim \pm 5 \mu\text{A}$. Preventing the flow of

current through the A- and B-nanostructures is probably due to the effect of the Coulomb blockade, which is removed with an increase in the bias voltage.

Further opening of the 1,3-CHD ring (C-, D-structure) leads to a significant reduction in the distance from the electrode surface to the molecule $\sim 2.5\text{--}2.1 \text{ \AA}$, which allows the leakage (tunneling) of electrons through the island molecule.

On the CVC of a C-nanodevice, in the intervals $-1.29 \div 0.91 \text{ V}$, $-0.58 \div 0.29 \text{ V}$ and $0.32 \div 0.8 \text{ V}$, sharp current drops are observed, which form sections of negative differential resistance (NDR). In the voltage range from -1.5 V to 0.85 V , strong current oscillations occur due to resonant tunneling of quasiparticles. These changes also appear on the dI/dV characteristic in the form of several resonant peaks of $12 \mu\text{S}$, $46.9 \mu\text{S}$, and $57.76 \mu\text{S}$ at bias voltages of -1.44 V , -0.75 V and 0 V , which demonstrates the strong effect of NDR (Fig. 6 b).

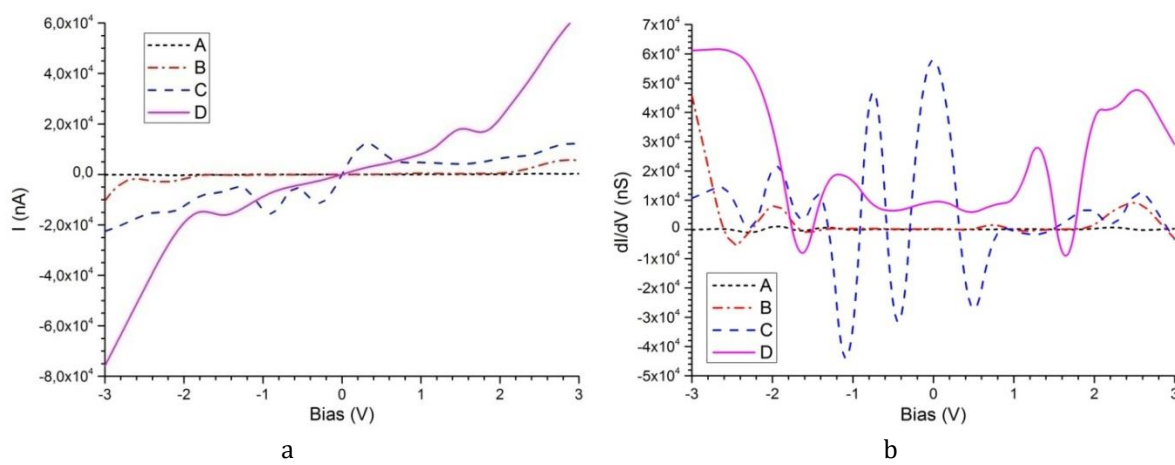


Figure 7. Current-voltage (a) and dI/dV characteristics (b) of nanodevices
 "Au – (1,3-CHD → 1,3,5-HT) – Au"

Oscillations of the characteristics are partially suppressed upon complete optimization of the 1,3-CHD molecule after ring opening and conversion to 1,3,5-HT (D-structure). In this case, the distance from the Au(111) surface to the 1,3,5-HT molecule is $\sim 2.1 \text{ \AA}$. On the CMC of the D-nanodevice, in the intervals of $-1.75 \div 1.5 \text{ V}$ and $1.53 \div 1.76 \text{ V}$, insignificant (in comparison with the characteristics of the C structure) current drops are observed, which form sections of the NDR. The differential conductivity and signals of the second derivative of the D-nanodevice resembles the characteristics of a two-mode phonon system with a symmetric term [48, 49] (Fig. 8).

In such systems, the conductivity increases (or decreases) due to phonon scattering. The peaks of the first mode of the d^2I/dV^2 characteristic of the nanodevice $-1.6 \cdot 10^5 \text{ nA/V}^2$ and $2.2 \cdot 10^5 \text{ nA/V}^2$ arise at a bias voltage of -1.8 V and 1.8 V , respectively, and the second mode is $-4 \cdot 10^4 \text{ nA/V}^2$ and $9 \cdot 10^4 \text{ nA/V}^2$ at a bias voltage of -0.9 V and 1.2 V . In [50], the interference effect is considered as one of the mechanisms responsible for the occurrence of NDR. However, the interference effect as a resonance phenomenon is suppressed by electron-phonon scattering. In our case, we believe that the disappearance on the electric transport characteristics of the D-nanodevice of explicit resonance effects is a suppression of resonant tunneling by the electron-phonon mechanism.

It should be noted that with the opening of the CHD ring, the slope of the CVC of nanodevices increases, which indicates a decrease in the electrical resistance of the molecule (Fig. 7a). Typically, such a change in the CVC occurs with increasing temperature of the system. In our case, one of the reasons for the temperature increase may be the heating of the phonon system [48].

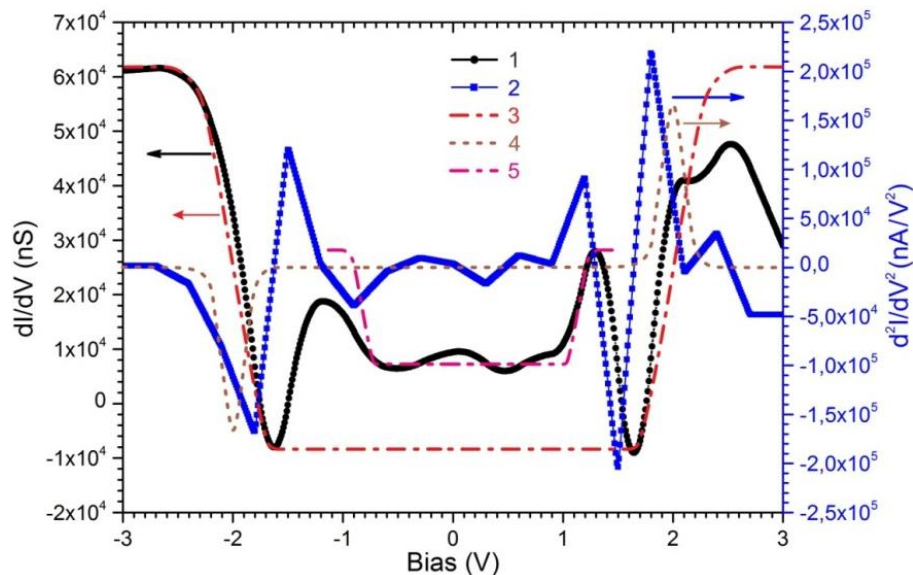


Figure 8. Phonon characteristics of a nanodevice “Au – 1,3,5-HT – Au” (D-configuration): 1 – differential conductivity of D-nanodevice, 2 – signals of the second derivative of the D-nanodevice, 3, 4 – dI/dV - and d^2I/dV^2 -characteristics of the phonon system with a symmetric term (first mode), respectively, 5 – dI/dV -characteristic of a phonon system with a symmetric term (second mode)

In [51, 52], it was found that NDR occurs only with one sign of the applied voltage, and at a different sign of the voltage this effect is absent. However, the possibility of the manifestation of NDR on both stress axes depends on the symmetry of the nanodevice molecule [53]. In our case, peaks and dips in the negative differential conductivity of the B- and C-nanostructures are observed on both semiaxes of the applied voltage due to the quasi-symmetric structure of the nanodevice, and in the C-nanodevice a significant NDR appears with a negative sign of the applied voltage due to the asymmetry of the C-configuration of the molecule.

We believe that ring breaking of a 1,3-CHD molecule can also occur from microwave radiation if the contacts are made of a superconducting material and the condition for the unsteady Josephson effect is fulfilled ($I > I_c$, where I is the transport current, I_c is the critical current). This would make it possible to create on their basis the basic logical gates AND, OR, NOT, functioning according to the classical electric circuit and controlled by the transport current.

4. CONCLUSION

Thus, in this work, we determined the main electric transport characteristics (DOS, transmission spectrum, CVC, dI/dV characteristics) of a nanoswitch consisting of Au(111) electrodes forming a nanogap of ~ 10.37 Å, where the 1,3-CHD molecule is located, with an external action of which opens its rings and turns into a 1,3,5-HT molecule. It was shown that the DOS of a nanodevice near the Fermi energy has a characteristic stable two-peak structure, as well as a decreasing peak at an energy of ~ -2.2 eV, associated with the opening of the CHD ring. An analysis of the transmission spectrum, CVC, and dI/dV characteristics revealed that the 1,3-CHD molecule weakly transmits electric current in the nanosystems under consideration than the 1,3,5-HT molecule. It is shown that the characteristics of the C-nanostructure are oscillatory in nature, associated with resonant tunneling of quasiparticles, which, after rectification, are suppressed possibly by electron-phonon scattering. The considered nanodevice can be used as a nanoswitch and nanosensor, as well as building blocks for creating logical elements in computer technology.

ACKNOWLEDGEMENTS

This work was supported by grant of the Ministry of Education and Science of the Republic of Kazakhstan AP08052562.

REFERENCES

- [1] Wang, J., Mu, X., Sun, M., Nanomaterials.vol.**9** (2019) pp.218.
- [2] Klinke, Ch., EPL.vol.**119**(2017) pp.36002.
- [3] Karmakar, S., Jain, F.C., Indian J. Phys. vol.**88**,issue12 (2014)pp.1275-1283.
- [4] Eslamia, L., Esmaeilzadeh, M., J. Appl. Phys. vol.**115**(2014) pp.084307.
- [5] Manimekalai, D., Dixit, P., Int. J. Nanoelectronics and Materials. vol. **10** (2017) pp.123-138.
- [6] Meymand, R.E., Soleymani, A., Granpayeh, N., Opt. Commun. vol.**458**(2020) pp.124772.
- [7] Goldooz, H., Badiei, A., Shiravand, G., Ghasemi, J.B., Ziarani G.M., J. Mater. Sci: Mater. Electron. vol. **30**(2019)pp. 17693-17705.
- [8] Cai, L., Zhang, S., Miao, J., Yu, Z., Wang, C., Adv. Funct. Mater. vol.**25**(2015) pp.5698-5705.
- [9] Dragoman, D., Dragoman, M., Physica E. vol. **33**(2006)pp.178-181.
- [10] Maligaspe, E., D'Souza, F., Org. Lett. vol. **12**, issue 3 (2010) 624-627.
- [11] Kanbara, T., Shibata, K., Fujiki, S., Kubozono, Y., Kashino, S., Urisu, T., Sakai, M., Fujiwara, A., Kumashiro, R., Tanigaki, K., Chem. Phys. Lett. vol. **379** (2003)pp.223-229.
- [12] Gentili, D., Sonar, P., Liscio, F., Cramer, T., Ferlauto, L., Leonardi, F., et al. Nano Lett. vol. **13**(2013) pp.3643.
- [13] Mukherjee, A., Saigal, N., Pandey, A., Nanotechnology. vol. **31**(2020) pp.055401.
- [14] Qi, S., Cunha, J., Guo, T-L., Chen, P., Zaccaria, R.P., Dai, M., Adv. Sci. vol. **7**, issue 6 (2019) pp.1901224.
- [15] Xiong, X., Huang, M., Hu, B., Li, X., Liu, F., Li, S., Tian, M., Li, T., Song, J., Wu, Y., Nat. Electron. vol. **3** (2020) pp.106-112.
- [16] Shin, G.H., Lee, G-B., An, E-S., Park, C., Jin, H.J., Lee, K.J., et al., ACS Appl. Mater. Interfaces. vol.**12**(2020) pp.5106-5112.
- [17] Nacak, H., Kusmartsev, F.V., Physica C. vol.**470**(2010) pp.827-831.
- [18] Takeuchi, N., Yamanashi, Y., Yoshikawa, N., Sci. Rep. vol. **4** (2015)pp.6354.
- [19] Liu, W-Y., Zheng, D-N., Zhao, S-P., Chin. Phys. B. vol. **27** (2018)pp.027401.
- [20] Zhou, Zh., Wu, H., Li, F., Ma, L., Qiao X., Dyes Pigments. vol. **174**(2020) pp.108033.
- [21] Kolodziejczyk, B., Ng, C.H., Strakosas, X., Malliaras, G.G., Winther-Jensen, B., Mater. Horiz. vol. **5**(2018)pp.93-98.
- [22] Chen, Q., Yoo, S-Y., Chung, Y-H., Lee, J-Y., Min, J., Choi, J-W., Bioelectrochemistry. vol.**111**(2016)pp.1-6.
- [23] .A.A. Shchuka, "Nanoelektronika", Moscow, Fizmatkniga,(2007) pp.464.

- [24] M. Joodaki, "Selected Advances in Nanoelectronic Devices", Heidelberg, New York, Dordrecht, London: Springer, (2013) pp.279.
- [25] Budyka, M.F., Russ. Chem. Rev. vol.**86**, issue 3 (2017) pp.181-210.
- [26] M. Kiguchi (Ed.), "Single-Molecule Electronics: An Introduction to Synthesis, Measurement and Theory", Singapore: Springer Science+Business Media, (2016) pp.235.
- [27] Sergeyev, D., J. Nano-Electron. Phys. vol. **11**, issue 6 (2019) pp.06022.
- [28] Sergeyev, D., Russ. Phys. J. vol. **59**, issue 3 (2016) pp.456-465.
- [29] Tuktarov, A.R., Khuzin, A.A., Dzhemilev, U.M., Russ. Chem. Rev. vol. **86** (6) pp. 474-509.
- [30] Wolf, T.J.A., Sanchez, D.M., Yang J., Parrish R.M., Nunes J.P.F., Centurion M., et al., Nature Chemistry. vol. 11 (2019) pp.504-509.
- [31] Minitti, M.P., Budarz, J.M., Kirrander, A., Robinson, J.S., Ratner, D., Lane, T.J., et al., Phys. Rev. Lett. vol. **114** (2015) pp.255501.
- [32] Arruda, B.C., Sension R.J., Phys. Chem. Chem. Phys. vol. **16** (2014) pp.4439.
- [33] Deb, S., Weber, P.M., Annu. Rev. Phys. Chem. vol. **62** (2011) pp.19-39.
- [34] Lei, Y., Wu, H., Zheng, X., Zhai, G., Zhu, C., J. of Photochemistry and Photobiology A: Chemistry. vol. **317** (2016) pp.39-49.
- [35] Tian, T., Xu, T., Kirk, S.R., Filatov, M., Jenkins, S., Int. J. Quantum Chem. vol. 119, issue 8 (2018) pp.e25862.
- [36] Jia, C., Migliore, A., Xin, N., Huang, S., Wang, J., Yang, Q., et al. Science. vol. **352**, issue 6292 (2016) pp.1443-1445.
- [37] Perdew, J.P., Burke, K., Ernzerhof, M., Phys. Rev. Lett. vol. **77** (1996) pp.3865.
- [38] N. Ferre, M. Filatov, M. Huix-Rotllant, (eds.), "Density-Functional Methods for Excited States", Switzerland: Springer International Publishing, (2016) pp. 481.
- [39] Stokbro, K., J. Phys.: Condens. Matter vol. **20** (2008) pp.064216.
- [40] Li, R., Zhang, J., Hou, S., Qian, Z., Shen, Z., Zhao, X., Xue, Z. Chemical Physics. vol. **336** (2007) pp.127-135.
- [41] Ganjia, M.D., Nourozi, F., Physica E. vol. **40** (2008) pp.2606-2613.
- [42] Smidstrup, S., Markussen, T., Vancraeyveld, P., Wellendorff, J., Schneider, J., Gunst, T., et al., J. Phys.: Condens. Matter vol. **32** (2020) pp.015901.
- [43] Sergeyev, D.M., Shunkeyev, K.S., Russ. Phys. J. vol. **60** (2018) pp.1938-1945.
- [44] Sergeyev, D.M., Tech. Phys. vol. **65**, issue 4 (2020) pp.573-577.
- [45] Sergeyev, D., Zhanturina, N., Radioengineering. vol. **28**, issue 4 (2019) pp.714-720.
- [46] Landauer, R., Philosophical Magazine. vol. **21**, issue 172 (1970) pp.863-867.
- [47] Datta, S., Nanotechnology. vol. **15** (2004) pp.S433.
- [48] Paulsson, M., Frederiksen, T., Brandbyge, M., Phys. Rev. B. vol. **72** (2005) pp.201101(R).
- [49] Paulsson, M., Frederiksen, T., Ueba, H., Lorente, N., Brandbyge, M., Phys. Rev. Lett. vol. **100** (2008) pp.226604.

- [50] Zhao, Y., Wan, Z., Xu, X., Patil, S.R., Hetmanuk, U., Anantram, M.P., Sci. Rep. vol.5(2015) pp.10712.
- [51] Guisinger, N.P., Greene, M.E., Basu, R., Baluch, A.S., Hersam, M.C., Nano Lett. vol.4(2004) pp.55-59.
- [52] Rakshit, T., Liang, G.Ch., Ghosh, A.W., Datta, S., Nano Lett. vol.4(2004) pp.1803.
- [53] Balashov, E.M., Budanov, B.A., Dalidchik, F.I., Kovalevskiy, S.A., JETP Letters. vol. **101** (2015) pp.643-647.

